PERGAMON

International Journal of Heat and Mass Transfer 44 (2001) 3443–3461

International Journal of HEAT and MASS TRANSFER

www.elsevier.com/locate/ijhmt

# Interfacial area concentration in steady fully-developed bubbly flow

Takashi Hibiki [a,1], Mamoru Ishii [b,*]

[a] Research Reactor Institute, Kyoto University, Kumatori-cho, Sennan-gun, Osaka 590-0494, Japan
[b] School of Nuclear Engineering, Purdue University, West Lafayette, IN 47907-1290, USA

Received 24 July 2000; received in revised form 27 November 2000

**Abstract**

Although bubbly flows are encountered in various engineering fields, there are very few established theoretical foundations on the interfacial area concentration, which have been supported by extensive experimental data. From this point of view, a simple equation for the interfacial area concentration under steady fully-developed bubbly flow condition has been derived from the interfacial area transport equation. The derived theoretical equation has been modified to obtain experimentally supported predictive correlation. The obtained interfacial area correlation was validated by 204 data sets measured in air–water bubbly flows under various conditions. These data sets covered extensive flow and loop conditions such as channel geometry (circular or rectangular channel), flow direction (vertical or horizontal flow), superficial gas velocity (0.018–4.87 m/s), superficial liquid velocity (0.262–6.55 m/s) and interfacial area concentration (25.8–1083 $m^{-1}$). An excellent agreement was obtained between the developed semi-theoretical correlation and data within an average relative deviation of ±11.1%. 

*Keywords:* Multiphase flow; Interfacial area concentration; Interfacial transfer term; Transport equation; Two-fluid model; Bubbly flow

## 1. Introduction

The basic structure of a bubbly two-phase flow can be characterized by two fundamental geometrical parameters. These are the void fraction and interfacial area concentration. The void fraction expresses the phase distribution and is a required parameter for hydrodynamic and thermal design in various industrial processes. On the other hand, the interfacial area describes available area for the interfacial transfer of mass, momentum and energy, and is a required parameter for a two-fluid model formulation. Various transfer mechanisms between phases depend on the two-phase interfacial structures. Therefore, an accurate knowledge of these parameters is necessary for any two-phase flow analyses. This fact can be further substantiated with respect to two-phase flow formulation.

In view of the great importance to two-fluid model, local measurements of these flow parameters such as void fraction and interfacial area concentration have been performed in a bubbly flow intensively over the past 10 years [1–12]. Some empirical correlations have been also proposed to predict volume-averaged interfacial area concentration over a section of a flow channel. Recently, Delhaye and Bricard [13] surveyed existing correlations on the interfacial area concentration extensively. They found that no existing correlations were satisfactory when compared with Bensler's extensive set of data [14], and proposed their own empirical correlation.

On the other hand, there are very few established theoretical foundations for relating the interfacial area concentration to some easily measurable quantities. Some investigators applied Kolmogoroff's theory of turbulence to obtain a semi-empirical model of the interfacial area concentration [15–20]. Even though their

* Corresponding author. Tel.: +1-765-494-4587; fax: +1-765-494-9570.

*E-mail addresses:* hibiki@rri.kyoto-u.ac.jp (T. Hibiki), ishii@ecn.purdue.edu (M. Ishii).

[1] Tel.: +81-724-51-2375; fax: +81-724-51-2461. Currently, adjunct associate professor of Faculty of Engineering Science, Osaka University.

0017-9310/01/$ - see front matter 
PII: S0017-9310(00)00365-3

**Nomenclature**

| | |
|---|---|
| $a$ | coefficient |
| $a_i$ | interfacial area concentration |
| $\tilde{a}_i$ | non-dimensional interfacial area concentration |
| $b$ | exponent |
| $C_0$ | distribution parameter |
| $c$ | ratio of the minimum eddy size, which would not cause bubble breakup, to the bubble diameter |
| $D_b$ | bubble diameter |
| $D_e$ | eddy diameter |
| $D_H$ | hydraulic equivalent diameter of the flow channel |
| $D_o$ | hole diameter |
| $(-dP/dz)_F$ | pressure loss per unit length due to friction |
| $f_f$ | friction factor of liquid phase |
| $G$ | mass flux |
| $g$ | gravitational acceleration |
| $j$ | mixture volumetric flux |
| $j_f$ | superficial liquid velocity |
| $j_g$ | superficial gas velocity |
| $j_{g,0}$ | superficial gas velocity at the inlet |
| $K_B$ | constant ($=1.59$) |
| $K_C$ | constant ($=1.29$ for an air–water system) |
| $Lo$ | Laplace length |
| $\tilde{Lo}$ | non-dimensional Laplace length |
| $N_t$ | number of bubbles passing the probe per unit time |
| $n$ | bubble number density |
| $n_o$ | hole area density on the perforated plate |
| $P$ | pressure |
| $Re_f$ | Reynolds number of liquid phase |
| $Re_g$ | Reynolds number of gas phase |
| $t$ | time |
| $V_{gj}$ | drift velocity |
| $v_g$ | gas velocity |
| $v_i$ | interfacial velocity |
| $v_p$ | average bubble velocity weighted by the bubble number |
| $v_r$ | relative velocity between gas and liquid phases |
| $v_{sz}$ | passing velocity of the interface through the double sensor probe |
| $We$ | Weber number |
| $z$ | axial position in the flow direction |

*Greek letters*

| | |
|---|---|
| $\alpha$ | void fraction |
| $\alpha_{max}$ | maximum allowable void fraction |
| $\beta$ | volumetric flow rate quality ($=j_{g,0}/j$) |
| $\gamma_B$ | adjustable parameter |
| $\gamma_C$ | adjustable parameter |
| $\Delta\rho$ | density difference |
| $\varepsilon$ | energy dissipation rate per unit mass obtained from the mechanical energy equation |
| $\tilde{\varepsilon}$ | non-dimensional energy dissipation rate per unit mass |
| $Z$ | coefficient |
| $\zeta$ | coefficient |
| $H$ | exponent to $\sigma/\rho_f$ |
| $\eta$ | exponent to $\sigma/\rho_f$ |
| $\Theta$ | exponent to $\alpha$ |
| $\theta$ | exponent to $\alpha$ |
| $\mu$ | liquid viscosity |
| $\nu_f$ | kinematic viscosity of liquid |
| $\xi$ | interfacial area concentration change due to bubble coalescence and breakup |
| $\rho_f$ | liquid density |
| $\rho_m$ | mixture density |
| $\sigma$ | surface tension |
| $\sigma_z$ | root mean square of the fluctuations of the $z$-component interfacial velocity |
| $X$ | exponent to $\varepsilon$ or $\tilde{\varepsilon}$ |
| $\chi$ | exponent to $\varepsilon$ |
| $\Phi_f^2$ | two-phase frictional multiplier based on pressure gradient of liquid flow |
| $\phi_B$ | increase rate of the bubble number density due to bubble breakup |
| $\phi_C$ | decrease rate of the bubble number density due to bubble coalescence |
| $\phi_{PC}$ | decrease rate of the bubble number density due to bubble collapse |
| $\phi_{PN}$ | increase rate of the bubble number density due to bubble nucleation |
| $\psi$ | factor depending on the shape of the bubbles ($=1/(36\pi)$ for spherical bubbles) |
| $\omega_0$ | maximum angle between the velocity vector of the interface and $z$-direction vector |

*Subscripts*

| | |
|---|---|
| calc. | calculated value |
| meas. | measured value |

*Mathematical symbol*

| | |
|---|---|
| $-t$ | time averaged quantity |

theoretical approach seemed convincing, the agreement with experimental data was often poor. Recently, some attempts have been made to obtain a theoretical foundation on the interfacial area. Kocamustafaogullari et al.

[5] concluded from a discussion on several bubble breakup mechanisms that average pressure fluctuations generated by the turbulent liquid fluctuations acting across a bubble diameter would be the only mechanism which would cause distortion of a bubble. Based on this force and the competing surface tension force, they developed a theoretical model for mean bubble size and interfacial area concentration. The theoretically predicted mean bubble size and interfacial area concentration were found to agree reasonably well with those measured in a horizontal bubbly flow. Millies et al. [21] derived the interfacial area concentration theoretically from the Boltzmann transport equation for the probability density function of the bubbles under steady fully-developed conditions. Millies and Mewes [22] also derived a simple equation for the interfacial area concentration from the population balance, taking into account the events of coalescence and bubble breakup for each bubble fraction. Their equation was validated by a large number of experimental data in bubble columns. However, there are still very few established theoretical foundations on the interfacial area concentration in a forced convective flow, which have been supported by extensive experimental data.

From this point of view, this paper aims to derive a simple equation for the interfacial area concentration from the interfacial area transport equation [23] under steady fully-developed flow condition. The derived theoretical equation is modified to obtain experimentally supported predictive correlation. The final equation is compared with experimental data of the interfacial area concentration in bubbly flows, which have been measured by various investigators.

## 2. Modeling of interfacial area concentration

### 2.1. Bubble number density and interfacial area transport equations

Recently, the interfacial area transport equation has been proposed to take into account the effect of entrance, developing flow, bubble breakup and coalescence, and wall nucleation source on the variation of the interfacial area concentration [24]. The one-dimensional bubble number density and interfacial area transport equations are given by Eqs. (1) and (2), respectively [23–25].

$$\frac{\partial n}{\partial t}+\frac{\mathrm{d}}{\mathrm{d}z}(nv_{\mathrm{p}})=(\phi_{\mathrm{B}}-\phi_{\mathrm{C}})+(\phi_{\mathrm{PN}}-\phi_{\mathrm{PC}}), \tag{1}$$

$$\frac{\partial a_{\mathrm{i}}}{\partial t}+\frac{\mathrm{d}}{\mathrm{d}z}(a_{\mathrm{i}}v_{\mathrm{i}}) =\frac{1}{3\psi}\left(\frac{\alpha}{a_{\mathrm{i}}}\right)^{2}\{(\phi_{\mathrm{B}}-\phi_{\mathrm{C}})+(\phi_{\mathrm{PN}}-\phi_{\mathrm{PC}})\} +\left(\frac{2a_{\mathrm{i}}}{3\alpha}\right)\left\{\frac{\partial\alpha}{\partial t}+\frac{\mathrm{d}}{\mathrm{d}z}(\alpha v_{\mathrm{i}})\right\}, \tag{2}$$

where $n$, $t$, $v_{\mathrm{p}}$, $z$, $a_{\mathrm{i}}$, $v_{\mathrm{i}}$, $\psi$, and $\alpha$ are the bubble number density, the time, the average bubble velocity weighted by the bubble number, the axial position along the flow direction ($z$-direction), the interfacial area concentration, the interfacial velocity, a factor depending on the shape of the bubbles ($\psi=1/(36\pi)$ for a spherical bubble), and the void fraction, respectively. $\phi_{\mathrm{B}}$, $\phi_{\mathrm{C}}$, $\phi_{\mathrm{PN}}$, and $\phi_{\mathrm{PC}}$ are the increase rate of the bubble number density due to bubble breakup, the decrease rate of the bubble number density due to bubble coalescence, the increase rate of the bubble number density due to bubble nucleation, and the decrease rate of the bubble number density due to bubble collapse, respectively.

Here, the fully-developed flow condition is defined as constant flux of bubble number density along the flow direction $\mathrm{d}(nv_{\mathrm{p}})\mathrm{d}z=0$. For steady fully-developed condition of an adiabatic flow ($\phi_{\mathrm{PN}}=0$, $\phi_{\mathrm{PC}}=0$), the bubble number density transport equation and the interfacial area transport equation are simplified as

$$\phi_{\mathrm{B}}-\phi_{\mathrm{C}}=0, \tag{3}$$

$$\frac{\mathrm{d}}{\mathrm{d}z}(a_{\mathrm{i}}v_{\mathrm{i}})=\left(\frac{2a_{\mathrm{i}}}{3\alpha}\right)\frac{\mathrm{d}}{\mathrm{d}z}(\alpha v_{\mathrm{i}}). \tag{4}$$

As can be clearly seen from Eq. (4), the interfacial area concentration is increased by the bubble expansion due to the pressure reduction along the flow direction even for the steady fully-developed flow condition defined in this study.

### 2.2. Modeling of increase and decrease rates of bubble number density

The increase rate of the bubble number density due to bubble breakup, $\phi_{\mathrm{B}}$, is given by the product of the bubble–eddy collision frequency and the breakup efficiency. They were modeled mechanistically in the previous paper [23]. The essential part of the model is summarized here. The bubble breakup is considered to occur due to the collision of the turbulent eddy with the bubble. For the estimation of bubble–eddy collision frequency, it is assumed that the eddies and bubbles behave like ideal gas molecules. Furthermore, the following assumptions are made for the modeling of the bubble–eddy collision frequency: (i) the turbulence is isotropic; (ii) the eddy size, $D_{\mathrm{e}}$, of interest lies in the inertial subrange; (iii) the eddy with the size from $c\cdot D_{\mathrm{b}}$ to $D_{\mathrm{b}}$ can break up the bubble with the size of $D_{\mathrm{b}}$, since larger eddies have the tendency to transport the bubble rather than to break it and smaller eddies do not have enough energy to break it. Following the kinetic theory of gases [26], the frequency of the collision between a single turbulent eddy and surrounding bubbles can be expressed by assuming the identical spherical bubbles and spherical eddies as a function of the surface available

to the collision and the volume available to the collision. In the derivation, the excluded volume for bubbles and eddies, and the overlap of the excluded volume for high void fraction region are also taken into account. On the other hand, the breakup efficiency can be derived from the relationship between the energy of a single eddy and the energy required for breakup [23,27]. Finally, the increase rate of the bubble number density due to bubble breakup, $\phi_B$, can be expressed as

$$\phi_B = \frac{\gamma_B \alpha(1-\alpha)\varepsilon^{1/3}}{D_b^{11/3}(\alpha_{max}-\alpha)} \exp\left(-\frac{K_B \sigma}{\rho_f D_b^{5/3}\varepsilon^{2/3}}\right), \tag{5}$$

where $\varepsilon$, $D_b$, $\alpha_{max}$, $K_B$, $\sigma$, and $\rho_f$ are the energy dissipation rate per unit mass, the bubble diameter, the maximum allowable void fraction ($=0.741$), the constant ($=1.59$), the surface tension, and the liquid density, respectively. $\gamma_B$ is an adjustable parameter to be determined experimentally.

The decrease rate of the bubble number density due to bubble coalescence, $\phi_C$, is given by the product of the bubble–bubble collision frequency rate and the coalescence efficiency. They were modeled mechanistically in the previous paper [23]. The essential part of the model is summarized here. The bubble coalescence is considered to occur due to the bubble random collision induced by turbulence in a liquid phase. For the estimation of bubble–bubble collision frequency, it is assumed that bubbles behave like ideal gas molecules in an isotropic turbulence system. Following the kinetic theory of gases [26], the frequency of the collision between a single bubble and surrounding bubbles can be expressed by assuming the identical spherical bubbles as a function of surface available to the collision and volume available to the collision. In the derivation, the excluded volume for bubbles, and the overlap of the excluded volume for high void fraction region are also taken into account. On the other hand, the coalescence efficiency can be derived from the liquid film-thinning model [28–30]. Finally, the decrease rate of the bubble number density due to bubble coalescence, $\phi_C$, can be expressed as

$$\phi_C = \frac{\gamma_C \alpha^2 \varepsilon^{1/3}}{D_b^{11/3}(\alpha_{max}-\alpha)} \exp\left(-\frac{K_C \rho_f^{1/2} D_b^{5/6}\varepsilon^{1/3}}{\sigma^{1/2}}\right), \tag{6}$$

where $\gamma_C$ and $K_C$ are an adjustable parameter to be determined experimentally and the constant ($=1.29$ for an air–water system), respectively.

### 2.3. Interfacial area concentration in steady fully-developed bubbly flow

The interfacial area concentration of the bubbly flow under steady fully-developed condition can be derived from Eqs. (3), (5) and (6) as

$$\begin{aligned} a_i &= \left[K_B\left\{1-\frac{K_C}{K_B}D_b^{2.5}\left(\frac{\sigma}{\rho_f}\right)^{-1.5}\varepsilon\right\}\right]^{-0.6} \\ &\quad \times \left[6\alpha\left\{\ln\frac{\gamma_B(1-\alpha)}{\gamma_C\alpha}\right\}^{0.6}\right]\left(\frac{\sigma}{\rho_f}\right)^{-0.6}\varepsilon^{0.4} \\ &\approx \varsigma\left[K_B\left\{1-\frac{K_C}{K_B}D_b^{2.5}\left(\frac{\sigma}{\rho_f}\right)^{-1.5}\varepsilon\right\}\right]^{-0.6} \\ &\quad \times \left(\frac{\sigma}{\rho_f}\right)^{-0.6}\alpha^{\theta}\varepsilon^{0.4}, \end{aligned} \tag{7}$$

where $\zeta$ and $\theta$ are a coefficient and an exponent to $\alpha$, respectively, when $6\alpha[\ln[\{\gamma_B(1-\alpha)\}/(\gamma_C\alpha)]]^{0.6}$ is approximated by $\zeta\alpha^{\theta}$. Considering the dependence of parameters in the first bracket of the right-hand side of Eq. (7), Eq. (7) may be further recast as

$$a_i \approx \varsigma'\left(\frac{\sigma}{\rho_f}\right)^{-\eta}\alpha^{\theta'}\varepsilon^{\chi}, \tag{8}$$

where $\zeta'$ is a coefficient, and $\eta$, $\theta'$ and $\chi$ are exponents to $(\sigma/\rho_f)$, $\alpha$ and $\varepsilon$, respectively.

For high energy dissipation rate per unit mass, Eq. (7) can be simplified as

$$\begin{aligned} a_i &= \left[6K_C^{1.2}\alpha\left\{\ln\frac{\gamma_C\alpha}{\gamma_B(1-\alpha)}\right\}^{-1.2}\right]\left(\frac{\sigma}{\rho_f}\right)^{-0.6}\varepsilon^{0.4} \\ &\approx \varsigma''\left(\frac{\sigma}{\rho_f}\right)^{-0.6}\alpha^{\theta''}\varepsilon^{0.4} \\ &\quad \text{for } \frac{K_C}{K_B}D_b^{2.5}\left(\frac{\sigma}{\rho_f}\right)^{-1.5}\varepsilon \gg 1, \end{aligned} \tag{9}$$

where $\zeta''$ and $\theta''$ are a coefficient and an exponent to $\alpha$, respectively, when $6K_C^{1.2}\alpha[\ln[(\gamma_C\alpha)/\{\gamma_B(1-\alpha)\}]]^{-1.2}$ is approximated by $\zeta''\alpha^{\theta''}$.

For low energy dissipation rate per unit mass, Eq. (7) can be simplified as

$$\begin{aligned} a_i &= \left[6K_B^{-0.6}\alpha\left\{\ln\frac{\gamma_B(1-\alpha)}{\gamma_C\alpha}\right\}^{0.6}\right]\left(\frac{\sigma}{\rho_f}\right)^{-0.6}\varepsilon^{0.4} \\ &\approx \varsigma'''\left(\frac{\sigma}{\rho_f}\right)^{-0.6}\alpha^{\theta'''}\varepsilon^{0.4} \\ &\quad \text{for } \frac{K_C}{K_B}D_b^{2.5}\left(\frac{\sigma}{\rho_f}\right)^{-1.5}\varepsilon \ll 1, \end{aligned} \tag{10}$$

where $\zeta'''$ and $\theta'''$ are a coefficient and an exponent to $\alpha$, respectively, when $6K_B^{-0.6}\alpha[\ln\{\gamma_B(1-\alpha)/(\gamma_C\alpha)\}]^{0.6}$ is approximated by $\zeta'''\alpha^{\theta'''}$.

## 3. Results and discussion

### 3.1. Existing interfacial area correlations and models

Existing interfacial area correlations and models are listed in Table 1. The correlations and models are recast

Table 1
Correlations and models of interfacial area concentration

| Investigators | Originally proposed correlations and models | Recast correlations with some assumptions |
|---|---|---|
| Hibiki and Ishii (present study) | $\tilde{a}_i = 0.500\tilde{L}o^{-0.283}\alpha^{0.847}\tilde{\varepsilon}^{0.283}$ or | $a_i = \{0.500(f_f\Phi_f^2 j_f^2)^{0.0707}\}g^{0.5}\frac{D_H^{0.212}}{\nu_f^{0.212}}\left(\frac{\sigma}{\Delta\rho}\right)^{-0.5}\alpha^{0.9}j_g^{0.0707}$ for $j_g \gg j_f$ |
| | $a_i = 0.500\frac{D_H^{0.283}}{\nu_f^{0.212}}\left(\frac{\sigma}{g\Delta\rho}\right)^{-0.5}\alpha^{0.847}\varepsilon^{0.0707}$ | $a_i = \{0.500(f_f\Phi_f^2)^{0.0707}\}g^{0.5}\frac{D_H^{0.212}}{\nu_f^{0.212}}\left(\frac{\sigma}{\Delta\rho}\right)^{-0.5}\alpha^{0.9}j_f^{0.212}$ for $j_f \gg j_g$ |
| Yun [8] | $a_i = \frac{1.72\beta^{0.81}}{(\sigma/\Delta\rho)^{0.5}}$ | $a_i \approx (1.72g^{0.5}C_0^{0.81})\left(\frac{\sigma}{\rho_f}\right)^{-0.5}\alpha^{0.81}$ for $\Delta\rho \approx \rho_f$, $C_0 j \gg V_{gj}$ |
| Millies et al. [21] | $a_i = 5.41\left(\frac{\sigma}{\rho_f}\right)^{-0.6}\alpha^{0.83}\varepsilon^{0.4}$ | $a_i = 5.41\left(\frac{\sigma}{\rho_f}\right)^{-0.6}\alpha^{0.83}\varepsilon^{0.4}$ |
| Kocamustafaogullari et al. [5] | $a_i = \frac{6\alpha\{j(-dP/dz)_F\}^{2/9}}{1.06(\sigma/\rho_f^{1/3})^{1/3}\{\alpha(1-\alpha)D_H^2\}^{2/9}}$ | $a_i = (5.66D_H^{-0.44})\left(\frac{\sigma}{\rho_f}\right)^{-0.33}\alpha^{0.78}\varepsilon^{0.22}$ |
| Zeitoun et al. [31] | $a_i = 3.24\alpha^{0.757}\left(\frac{g\Delta\rho}{\sigma}\right)^{0.55}\left(\frac{\mu_f}{G}\right)^{0.1}$ | $a_i \approx (3.24g^{0.55}\mu_f^{0.1})\left(\frac{\sigma}{\rho_f}\right)^{-0.55}\alpha^{0.757}G^{-0.1}$ for $\Delta\rho \approx \rho_f$ |
| Delhaye and Bricard [13] | $a_i = \left(\frac{\sigma}{g\Delta\rho}\right)^{-0.5}\left(7.23 - \frac{6.82Re_f}{Re_f + 3240}\right) \times 10^{-3}Re_g$ | $a_i \approx g^{0.5}\left(\frac{\sigma}{\rho_f}\right)^{-0.5}\left(7.23 - \frac{6.82Re_f}{Re_f + 3240}\right) \times 10^{-3}Re_g$ for $\Delta\rho \approx \rho_f$ |
| MINI-TRAC as in Hori and Toda [32] | $a_i = \frac{6\alpha\rho_f v_r^2}{We\sigma}$ where $We = 7.5$ | $a_i = \left(\frac{6}{We}\right)\left(\frac{\sigma}{\rho_f}\right)^{-1}\alpha v_r^2$ where $We = 7.5$ |
| Tabei et al. [33] | $a_i = 2100\alpha^{1.25}(1-\alpha)^{0.75}$ | $a_i \approx 945\alpha^{0.847}$ |
| Serizawa and Kataoka [1] | $a_i = 1030\alpha^{0.87}j_f^{0.2}$ | $a_i = 1030\alpha^{0.87}j_f^{0.2}$ |
| Fukuma et al. [34] | $a_i = 300\alpha$ | $a_i = 300\alpha$ |
| Viswanathan [35] | $a_i = \frac{6\alpha}{\ln(7.768j_g^{0.26})\left(\frac{\sigma^3}{\rho_f^3 g^2 j_g^2}\right)^{0.2}}$ | $a_i = (6g^{0.1})\left(\frac{\sigma}{\rho_f}\right)^{-0.6}\alpha\left\{\frac{j_g^{0.1}}{\ln(7.768j_g^{0.26})}\right\} \approx (2.82g^{0.1})\left(\frac{\sigma}{\rho_f}\right)^{-0.6}\alpha j_g^{-0.085}$ |
| Trambouze et al. [36] | $a_i = a\left\{j_g\left(-\frac{dP}{dz}\right)_T\right\}^b$ | $a_i = a\left\{j_g\left(-\frac{dP}{dz}\right)_T\right\}^b$ |

(continued on next page)

Table 1 (*continued*)

| Investigators | Originally proposed correlations and models | Recast correlations with some assumptions |
|---|---|---|
| Calderbank [15]; Burgess and Calderbank [16–18]; de Figueiredo and Calderbank [19]; Chandrasekharan and Calderbank [20] | $a_i \approx \left(\frac{\sigma}{\rho_f}\right)^{-0.6} \alpha^{\xi''''} \varepsilon^{0.4}$ | $a_i \approx \left(\frac{\sigma}{\rho_f}\right)^{-0.6} \alpha^{\xi''''} \varepsilon^{0.4}$ |
| TRAC-P1A as in Kelly and Kazimi [37] | $a_i = \frac{6\alpha\rho_f v_r^2}{We\sigma}$ where $We = 50$ | $a_i = \left(\frac{6}{\alpha}\right)\left(\frac{\sigma}{\rho_f}\right)^{-1} \alpha v_r^2$ where $We = 50$ |
| Tomida et al. [38] | $a_i = \frac{2}{a'\rho_g} \alpha j_g^{-(b'+2)} \left(-\frac{dP}{dz}\right)_T$ | $a_i = \frac{2}{a'\rho_g} \alpha j_g^{-(b'+2)} \left(-\frac{dP}{dz}\right)_T$ |
| Kasturi and Stepanek [39]; Shilimkan and Stepanek [40] | $a_i = a'' \frac{1-\alpha}{Q_f} \left(-\frac{dP}{dz}\right)_F^{b''}$ | $a_i = a'' \frac{1-\alpha}{Q_f} \left(-\frac{dP}{dz}\right)_F^{b''}$ |
| Akita and Yoshida [41] | $a_i = \left\{0.23 g^{0.56} D_H^{0.3} \left(\frac{\rho_f}{\mu_f}\right)^{0.24}\right\} \left(\frac{\sigma}{\rho_f}\right)^{-0.5} \alpha j_g^{0.12}$ | $a_i = \left\{0.23 g^{0.06} D_H^{0.3} \nu_f^{-0.24}\right\} \left(\frac{\sigma}{g\rho_f}\right)^{-0.5} \alpha j_g^{0.12}$ |
| Japsen [42] | $a_i = a''' \left\{ j \left(-\frac{dP}{dz}\right)_F \right\}^{b'''}$ | $a_i = a''' \left\{ j \left(-\frac{dP}{dz}\right)_F \right\}^{b'''}$ |
| Banerjee [43] | $a_i = a'''' \left\{ Q_f \left(-\frac{dP}{dz}\right)_F \right\}^{b''''}$ | $a_i = a'''' \left\{ Q_f \left(-\frac{dP}{dz}\right)_F \right\}^{b''''}$ |
| Calderbank [44] | $a_i = 0.38 \left(\frac{j_g}{v_g}\right)^{0.775} \left\{\frac{\rho_f j_g}{n_o D_o \mu_f}\right\}^{0.125} \left(\frac{g\rho_f}{D_o\sigma}\right)^{1/3}$ | $a_i = \left[0.38 \left(\frac{g}{D_o}\right)^{0.33} \left\{\frac{\rho_f}{n_o D_o \mu_f}\right\}^{0.125}\right] \left(\frac{\sigma}{\rho_f}\right)^{-0.33} \alpha^{0.775} j_g^{0.125}$ |

for further discussion on the dependence of flow parameters such as $(\sigma/\rho_f)$, $\alpha$ and $\varepsilon$ on the interfacial area concentration. Interestingly, most of the interfacial area correlations and models have the following functional form:

$$a_i = Z\left(\frac{\sigma}{\rho_f}\right)^{-H}\alpha^{\Theta}\varepsilon^{X} \quad \text{or} \quad a_i = Z\left(\frac{\sigma}{\Delta\rho}\right)^{-H}\alpha^{\Theta}\varepsilon^{X}, \tag{11}$$

where $Z$ is a coefficient, and $H$, $\Theta$ and $X$ are exponents to $(\sigma/\rho_f)$ or $(\sigma/\Delta\rho)$, $\alpha$ and $\varepsilon$, respectively. Since $\Delta\rho$ is nearly equal to $\rho_f$ for most gas–liquid bubbly flows, this functional form agrees with Eq. (8), which is derived semi-theoretically from the interfacial area transport equation. Superficial gas and liquid velocities are found in some interfacial area correlations instead of the energy dissipation rate per unit mass. This can be explained as follows. Here, the energy dissipation rate per unit mass is simply given from the mechanical energy equation as [5,23]:

$$\varepsilon = \frac{j}{\rho_m}\left(-\frac{dP}{dz}\right)_F, \tag{12}$$

where $j$, $\rho_m$, and $(-dP/dz)_F$ refer to the mixture volumetric flux, the mixture density, and the pressure loss per unit length due to friction, respectively. The pressure loss per unit length due to friction can be calculated from Lockhart–Martinelli's correlation [45]. Substituting Eq. (12) into Eq. (11) yields

$$a_i = Z'\left(\frac{\sigma}{\rho_f}\right)^{-H}\frac{\alpha^{\Theta}}{(1-\alpha)^{X}}\left\{\frac{f_f\Phi_f^2}{D_H}(j_g+j_f)j_f^2\right\}^{X}, \tag{13}$$

where $Z'$, $f_f$, $\Phi_f^2$, $D_H$, $j_g$, and $j_f$ are a coefficient, the friction factor of liquid phase, the two-phase frictional multiplier based on pressure gradient of liquid flow, the hydraulic equivalent diameter of the flow channel, the superficial gas velocity and the superficial liquid velocity, respectively. The above equation can be approximated for two extreme conditions as

$$a_i = Z''\left\{\frac{f_f\Phi_f^2}{D_H}j_f^2\right\}^{X}\left(\frac{\sigma}{\rho_f}\right)^{-H}\alpha^{\Theta'}j_g^{X} \quad \text{for } j_g \gg j_f, \tag{14}$$

$$a_i = Z''\left\{\frac{f_f\Phi_f^2}{D_H}\right\}^{X}\left(\frac{\sigma}{\rho_f}\right)^{-H}\alpha^{\Theta'}j_f^{3X} \quad \text{for } j_g \ll j_f, \tag{15}$$

where $Z''$ and $\Theta'$ are a coefficient and an exponent to $\alpha$, respectively, when $\alpha^{\Theta}/(1-\alpha)^{X}$ is approximated by $Z'''\alpha^{\Theta'}$.

Table 2 shows a list of exponents to $(\sigma/\rho_f)$, $\alpha$, and $\varepsilon$ (or $j_g$, $j_f$ or $G$ (mass flux)) in the existing interfacial area correlations and models. The exponent to $(\sigma/\rho_f)$ or $(\sigma/\Delta\rho)$ ranges from 0.33 to 0.6, and the exponent to $\alpha$ is about 0.8. It can be concluded from the above discussions that Eq. (8) derived semi-theoretically from the interfacial area transport equation is promising for correlating the interfacial area concentration.

### 3.2. Database for development of interfacial area correlation

The database used for the development of the interfacial area correlation for steady fully-developed bubbly flows is listed in Table 3. If axial changes of the interfacial area concentration and the pressure are available, one can identify the data set, which represent the fully-developed bubbly flow. In Fig. 1, the ratio of measured interfacial area concentration to interfacial area concentration calculated from the pressure drop under the assumption of equilibrium state of bubble breakup and

Table 2
Exponents to parameters appeared in correlations and models of interfacial area concentration

| Investigators | Exponent to $(\sigma/\rho_f)$ or $(\sigma/\Delta\rho_f)$ | Exponent to $\alpha$ | Exponent to $\varepsilon$, $j_g$, $j_f$, or $G$ |
|---|---|---|---|
| Hibiki and Ishii (present study) | −0.5 | 0.847 | $0.0707(\varepsilon)$<br>$0.0707(j_g)$<br>$0.212(j_f)$ |
| Yun [8] | −0.5 | 0.81 | $0(\varepsilon)$ |
| Millies et al. [21] | −0.6 | 0.83 | $0.4(\varepsilon)$ |
| Kocamustafaogullari et al. [5] | −0.33 | 0.78 | $0.22(\varepsilon)$ |
| Zeitoun et al. [31] | −0.55 | 0.757 | $-0.1(G)$ |
| Tabei et al. [33] | – | 0.847 | $0(\varepsilon)$ |
| Serizawa and Kataoka [1] | – | 0.87 | $0.2(j_f)$ |
| Fukuma et al. [34] | – | 1 | $0(\varepsilon)$ |
| Viswanathan [35] | −0.6 | 1 | $-0.085(j_g)$ |
| Calderbank [15]; Burgess and Calderbank [16–18]; de Figueiredo and Calderbank [19]; Chandrasekharan and Calderbank [20] | −0.6 | $\theta$ | $0.4(\varepsilon)$ |
| Akita and Yoshida [41] | −0.5 | 1 | $0.12(j_g)$ |
| Calderbank [44] | −0.33 | 0.775 | $0.125(j_g)$ |

Table 3
Database used for the development of interfacial area correlation

| Investigators | Geometry (mm) | Flow direction | Gas | Liquid | $z/D$ (no dimension) | Pressure (MPa) | Superficial gas velocity (m/s) | Superficial liquid velocity (m/s) | Interfacial area concentration ($m^{-1}$) | Number of data | Technique |
|---|---|---|---|---|---|---|---|---|---|---|---|
| Hibiki and Ishii [12] | 25.4 ID pipe | Vertical | Air | Water | 125 | 0.10 | 0.0566–1.27 | 0.262–3.49 | 40.5–551 | 25 | Probe |
| Hibiki et al. [11] | 50.8 ID pipe | Vertical | Air | Water | 54 | 0.10 | 0.0358–4.87 | 0.491–5.00 | 101–1083 | 18 | Probe |
| Hibiki et al. [10] | 50.8 ID pipe | Vertical | Air | Water | 62 | 0.10 | 0.0178–0.0936 | 0.60–1.30 | 25.8–135 | 9 | Probe |
| Yun [8] | Annulus, $D_H = 17$ | Vertical | Steam | Water | 94 | 0.10, 0.71 | 0.00290–0.138 | 0.456–1.79 | 11.6–161 | 49 | Probe |
| | Bundle $(2 \times 2),\ 36.2(D_H)$ | Vertical | Steam | Water | 44 | 0.10, 0.71 | 0.0122–0.156 | 0.247–0.786 | 20.0–247 | 46 | Probe |
| | Bundle $(3 \times 3),\ 8.59(D_H)$ | Vertical | Steam | Water | 186 | 0.10 | 0.00580–0.0896 | 0.261–0.630 | 35.6–290 | 58 | Probe |
| Grossetete [7] | 38.1 ID pipe | Vertical | Air | Water | 155 | 0.10 | 0.0895–0.181 | 0.877–1.75 | 75.1–145 | 3 | Probe |
| Kocamustafaogullari et al. [5] | 50.3 ID pipe | Horizon-tal | Air | Water | 253 | 0.10 | 0.212–1.35 | 3.74–6.55 | 124–507 | 52 | Probe |
| Kalkach-Navarro [4] | 38.1 ID pipe | Vertical | Air | Water | 50 | 0.10 | 0.056–0.332 | 0.30–1.25 | 93.4–298 | 17 | Probe |
| Serizawa et al. [3] | 30.0 ID pipe | Vertical | Air | Water | 83 | 0.10 | 0.018–0.54 | 0.50–5.0 | 53.2–338 | 22 | Probe |
| Bensler [14] | $40 \times 40$ | Vertical | Air | Water | 65 | 0.10 | 0.035–0.253 | 0.503–3.00 | 67.0–391.6 | 16 | Photographic |
| Liu [2] | 38.1 ID pipe | Vertical | Air | Water | 36 | 0.10 | 0.027–0.347 | 0.376–1.39 | 38.2–591 | 42 | Probe |

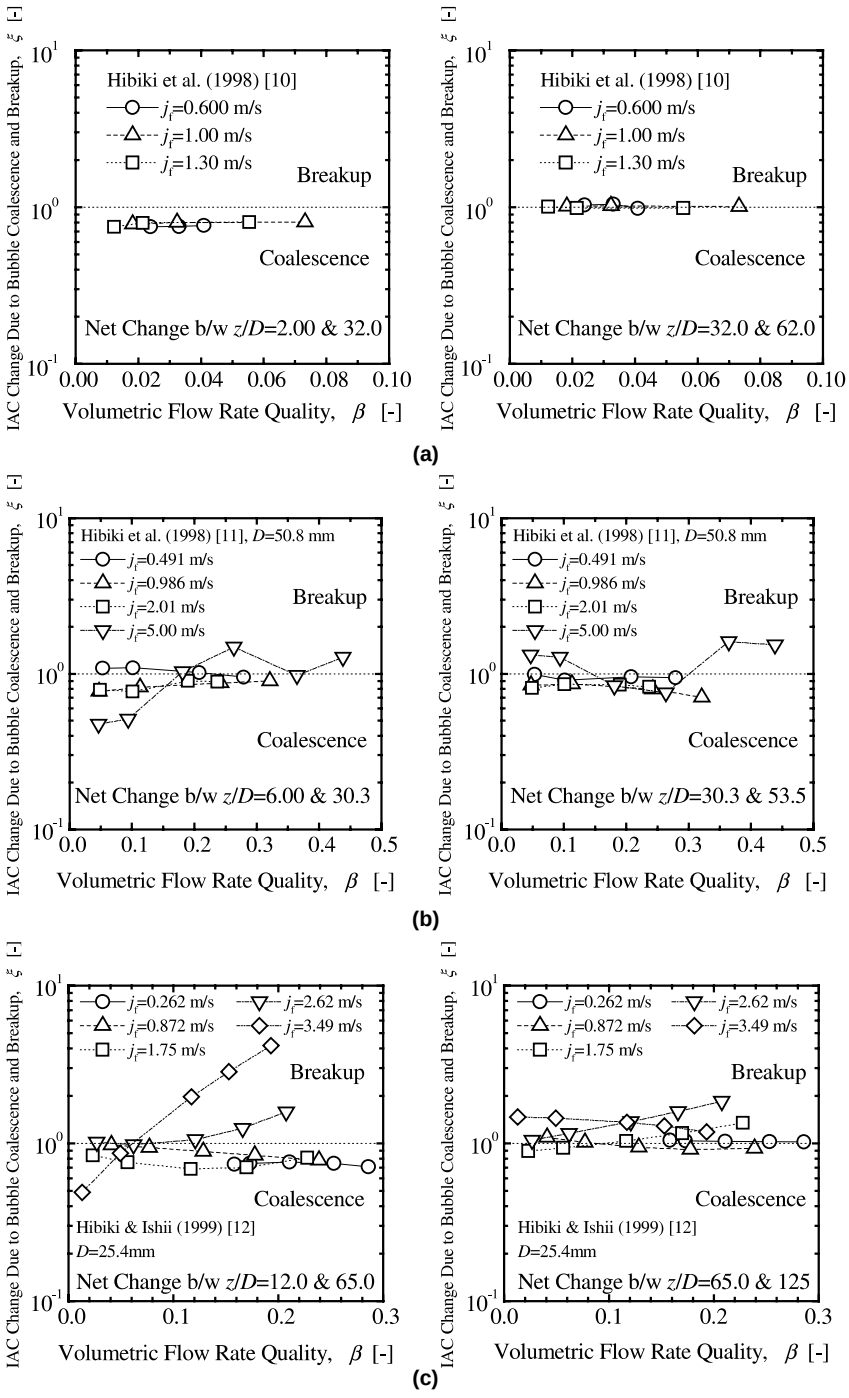


Fig. 1. Interfacial area concentration change due to buble breakup and coalescence: (a) data by Hibiki et al. [10]; (b) data by Hibiki et al. [11]; (c) data by Hibiki and Ishii [12].

coalescence rates, $\xi$, is plotted against volumetric flow rate quality, $\beta\ (=j_{g,0}/(j_{g,0}+j_f))$. The parameter, $\xi$, represents the change in the interfacial area concentration only due to bubble breakup or coalescence [10–12]. $\xi > 1$ or $\xi < 1$ indicates that the bubble breakup or coalescence is dominant, respectively. Figs. 1(a)–(c) show the calculated results for (a) the data taken at low void fraction region ($\alpha \leqslant 10\%$) in $D = 50.8$ mm pipe [10],

(b) the data taken in $D = 50.8$ mm pipe [11], and (c) the data taken in $D = 25.4$ mm pipe [12], respectively. In these data sets, the measurements of flow parameters were performed at three axial locations. The left and right figures in Fig. 1 depict the calculated results between the first and second measuring stations, and between the second and third measuring stations, respectively. As shown in Fig. 1(a), $\xi$-value is about 1 for the $a_i$ change between $z/D = 32$ and 62. This suggests that the flow conditions of data shown in Fig. 1(a) can be considered to be fully-developed flow at $z/D = 32$. On the other hand, comparing right figure with left figure in Figs. 1(b) and (c), $\xi$-values tend to collapse on the line of $\xi = 1$ along the axial direction. This tendency would be further emphasized at the downstream of the third measuring station. Therefore, it may be considered that the flow conditions of data sets shown in Fig. 1 are quasi fully-developed bubbly flow condition at the third measuring station.

Since axial changes of the interfacial area concentration and the pressure are not available in most of data sets listed in Table 3, the identification of the data set indicating the fully-developed bubbly flow cannot be performed for the data sets besides those shown in Fig. 1 quantitatively. Instead, some investigators listed in Table 3 suggested that their data were taken under the fully-developed bubbly flows qualitatively. Kocamustafaogullari et al. [5] explained that their experiments were carried out at $z/D = 253$ ($D = 50.3$ mm) under fully-developed bubbly flow conditions. Kalcach-Navarro [4] also stated that the dual-sensor resistivity probe was located at $z/D = 50$ ($D = 38.1$ mm) to allow for fully-developed two-phase flow. Therefore, it may be concluded that the flow conditions of the data sets listed in Table 3 can be accepted as quasi fully-developed flows. However, in a strict sense, it should be pointed out that the correlation of the interfacial area concentration to be developed might include a little effect of developing flow.

In the photographic method, the interfacial area concentration is directly calculated from the image, whereas in the double sensor probe method, the interfacial area concentration are calculated by interpreting the number of bubbles hitting a probe per unit time and the gas velocity with help of a theoretical model. Different investigators adopt different theoretical models. For consistency, the time-averaged interfacial area concentrations used for the development of the interfacial area correlation are recalculated by using the following equation [10] with the data of the number of bubbles hitting a probe per unit time and the gas velocity, which were obtained by various investigators.

$$a_i = 2N_t \overline{\frac{1}{v_{sz}}}^t I(\omega_0), \quad I(\omega_0) = \frac{\omega_0^3}{3(\omega_0^3 - \sin\omega_0)}, \tag{16}$$

where $N_t$, $v_{sz}$, and $\omega_0$ are the number of bubbles which pass the point per unit time, the passing velocity of the interface through the double sensor probe in the $z$-direction, and the maximum angle between the velocity vector of the interface and $z$-direction vector, respectively. $-t$ means the time-averaged quantity. The relationship between the maximum angle and the interfacial velocity is given by

$$\frac{3}{2\omega_0^2}\left(1 - \frac{\sin 2\omega_0}{2\omega_0}\right) = \frac{1 - (\sigma_z^2/v_{sz}^2)}{1 + 3(\sigma_z^2/v_{sz}^2)}, \tag{17}$$

where $\sigma_z$ is the root-mean-square of the fluctuations of the $z$-component interfacial velocity. The interfacial area concentrations obtained by the probe method with Eqs. (16) and (17) agreed with those measured by the photographic method within an average relative deviation of $\pm 6.95\%$ [10].

### 3.3. Development of interfacial area correlation

In this section, the correlation of the interfacial area concentration under steady fully-developed bubbly flow is developed by the functional form represented by Eq. (8), and the existing database. Prior to the development of the correlation of the interfacial area concentration, Eq. (8) may be non-dimensionalized by Kolmogoroff length scale [46] and Laplace length (or capillary length), $Lo$ defined by $\sqrt{\sigma/g\Delta\rho}$ as follows.

$$\tilde{a}_i = Z'''\alpha^{\Theta''}\tilde{\varepsilon}^{X'},$$

where

$$\tilde{a}_i \equiv \frac{a_i}{Lo^{-1}} \quad \text{and} \quad \tilde{\varepsilon} \equiv Lo\left(\frac{\varepsilon}{v_f^3}\right)^{1/4}. \tag{18}$$

Here, $Z'''$ and $v_f$ are a coefficient and the kinematic viscosity, respectively, and $\Theta''$ and $X'$ are exponents to $\alpha$ and $\tilde{\varepsilon}$, respectively. It should be noted here that the term of $(\sigma/\rho_f)$ does not appear in Eq. (18) explicitly. As explained in Section 3.2, since only air–water flow data are available for developing the correlation of the interfacial area concentration, the dependence of physical properties such as $(\sigma/\rho_f)$ on the interfacial area concentration may not be completely included in the correlation to be developed. Thus, the coefficient $Z'''$ may be a function of $(\sigma/\rho_f)$. As will be discussed later, the dependence will be examined by introducing a non-dimensional term such as $Lo/D_H$ into the correlation. However, in Eq. (18), the dependence of the surface tension and fluid density on the interfacial area concentration may be partly counted by Laplace length.

The coefficient and the exponents to $\alpha$ and $\tilde{\varepsilon}$ are determined to be 1.08, 0.847, and 0.283, respectively, by the least-squares method with 204 data taken in air–water bubbly flows listed in Table 3. Finally, the developed interfacial area correlations for adiabatic air–water

bubbly flow under steady fully-developed condition is expressed as

$$\tilde{a}_i = 1.08\alpha^{0.847}\tilde{\varepsilon}^{0.283} \quad \text{or}$$
$$a_i = 1.08 v_f^{-0.212}\left(\frac{\sigma}{g\Delta\rho}\right)^{-0.359}\alpha^{0.847}\varepsilon^{0.0707}. \tag{19}$$

As can be seen from Table 2, the obtained exponent to $\alpha$ ($= 0.847$) is similar to those reported by various investigators. The obtained exponent to $\sigma/\Delta\rho$ ($= -0.359$) is also in the range of the exponent reported by various investigators. The change of $(\sigma/\Delta\rho)^{-H}$ for $\sigma/\Delta\rho$ change is a weak function of the exponent to $\sigma/\Delta\rho$. For example, the difference in the value between $(\sigma/\Delta\rho)^{-0.5}$ and $(\sigma/\Delta\rho)^{-0.359}$ is within $\pm 5\%$ for $\pm 30\%$ change of $\sigma/\Delta\rho$, corresponding to $\sigma/\Delta\rho$ change for increasing water temperature from 20°C to 160°C. This means that a little difference in the exponent to $\sigma/\Delta\rho$ may not affect the predicted interfacial area concentration significantly. As discussed before, Eq. (18) does not count the dependence of the surface tension and fluid density on the interfacial area concentration explicitly. However, as a consequence, Eq. (19) may characterize the dependence adequately, though a slight modification on the dependence of physical properties may be needed.

From the detailed length scale consideration, the interfacial area concentration representing the interface structure length scale would be characterized by the space probability such as the void fraction, the system length scale such as the hydraulic equivalent diameter of the flow channel, the internal length scale such as the Laplace length, and the parameter characterizing the flow such as the energy dissipation rate per unit length. This suggests the following functional form to correlate the interfacial area concentration under steady fully-developed bubbly flow:

$$\tilde{a}_i = Z''''\tilde{L}o^{H'}\alpha^{\Theta''}\tilde{\varepsilon}^{X'},$$

where

$$\tilde{L}o \equiv \frac{Lo}{D_H}. \tag{20}$$

Here, $Z''''$ is a coefficient and $H'$ is an exponent to $\tilde{L}o$. Eq. (20) would be suitable for the functional form of the interfacial area concentration, since it includes the space probability, the three length scales and the parameter characterizing the flow. It should be noted here that not the term of $(\sigma/\rho_f)$ suggested by Eq. (8) but the term of $(\sigma/\Delta\rho)$ only appears in Eq. (20). Since the term of $\sqrt{\sigma/g\Delta\rho}$ has a clear physical meaning such as the internal length scale characterizing the bubble size length scale, the term of $(\sigma/\Delta\rho)$ would be much suitable rather than the term of $(\sigma/\rho_f)$ particularly for a boiling flow system. As already mentioned in Section 3.1, $\Delta\rho$ is nearly equal to $\rho_f$, which means that such modification on the term of $(\sigma/\rho_f)$ in Eq. (20) may not practically affect the prediction of the interfacial area concentration for most gas–liquid bubbly flow.

Since the exponents of $\Theta''$ and $X'$ are 0.847 and 0.283, respectively, $H'$ should be given in some ways. Here, Eq. (20) can be recast as follows:

$$a_i = \frac{Z''''}{D_H^{H'} v_f^{0.212}}\left(\frac{\sigma}{g\Delta\rho}\right)^{0.5(H'-0.717)}\alpha^{0.847}\varepsilon^{0.0707}. \tag{21}$$

As can be seen in Table 2, since the exponent to $(\sigma/\rho_f)$ or $(\sigma/\Delta\rho)$ in the empirical correlations of the interfacial area concentration is about $-0.5$, the exponent to $(\sigma/\Delta\rho)$ in Eq. (21) may be assumed to be $-0.5$. This exponent is quite similar to the analytical value for the case of very high or very low energy dissipation rate per unit mass (see Eqs. (9) and (10)). Finally, the coefficient, $Z''''$, is determined to be 0.500 by the least-squares method with 204 data sets. Thus, one can obtain the following correlation of the interfacial area concentration:

$$\tilde{a}_i = 0.500\tilde{L}o^{-0.283}\alpha^{0.847}\tilde{\varepsilon}^{0.283} \quad \text{or}$$
$$a_i = 0.500\frac{D_H^{0.283}}{v_f^{0.212}}\left(\frac{\sigma}{g\Delta\rho}\right)^{-0.5}\alpha^{0.847}\varepsilon^{0.0707}. \tag{22}$$

Eq. (22) should be verified by using rigorous data sets taken under various experimental conditions, particularly, various channel size conditions. It should be noted here that Eq. (22) gives a good prediction of the interfacial area concentration on the order of the prediction error by Eq. (19) for the tested data sets.

For $j_g \gg j_f$, Eq. (22) can be further recast as follows:

$$a_i = \left\{0.500(f_f\Phi_f^2 j_f^2)^{0.0707}\right\} g^{0.5}\frac{D_H^{0.212}}{v_f^{0.212}}\left(\frac{\sigma}{\Delta\rho}\right)^{-0.5}\alpha^{0.9} j_g^{0.0707}. \tag{23}$$

Here, $\alpha^{0.847}/(1-\alpha)^{0.0707}$ is approximated to be $\alpha^{0.9}$. Interestingly, this correlation is quite similar to the following correlation by Akita and Yoshida [41], which was developed for various systems such as water–air (or oxygen), glycol–air (or oxygen), methanol–air (or oxygen), and carbon tetrachloride–air in bubble columns with stagnant fluid.

$$a_i = 0.23 g^{0.56}\frac{D_H^{0.3}}{v_f^{0.24}}\left(\frac{\sigma}{\rho_f}\right)^{-0.5}\alpha j_g^{0.12}. \tag{24}$$

Interestingly, the exponents to $g$ ($= 0.5$), $D_H$ ($= 0.212$), $v_f$ ($= -0.212$), $\alpha$ ($= 0.9$), and $j_g$ ($= 0.0707$) in Eq. (23) are very similar to those to $g$ ($= 0.56$), $D_H$ ($= 0.3$), $v_f$ ($= -0.24$), $\alpha$ ($= 1$), and $j_g$ ($= 0.12$) in the empirical correlation by Akita and Yoshida [41], namely, Eq. (24).

For $j_g \ll j_f$, the exponent to $\varepsilon$ ($= 0.0707$) would correspond to a third of the exponent to $j_f$ ($= 0.212$),

see Eq. (15). It turns out that the obtained correlation, Eq. (22), is very similar to the following correlation proposed by Serizawa and Kataoka [1] for an air–water flow in a pipe ($D = 30$ mm):

$$a_i = 1030\alpha^{0.87} j_f^{0.2}. \quad (25)$$

It should be noted here that Eq. (25) is only applicable to the flow condition of $j_f \geqslant 1$ m/s. Serizawa and Kataoka [1] reported that for a low liquid flux ($j_f \leqslant 1$ m/s) the dependence of the interfacial area concentration on the liquid flux was reversed and their data were not successfully correlated by Eq. (25). On the other hand, Eq. (22) can be applied to the flow condition of $j_f \leqslant 1$ m/s as well as $j_f \geqslant 1$ m/s.

### 3.4. Comparison of developed interfacial area correlation with database

In this section, the developed interfacial area correlation, Eq. (22), is compared with each data listed in Table 3. Interfacial area models proposed by Kocamustafaogullari et al. [5] and Millies et al. [21], which were derived theoretically, are also compared with the data.

Figs. 2–10 show the comparison of the interfacial area correlation developed in this study, Eq. (22), with each data taken by each investigator. No significant deviations are found between Eq. (22) and each data regardless of channel geometry (circular or rectangular channel), flow direction (vertical or horizontal flow), superficial gas velocity (0.018–4.87 m/s), superficial

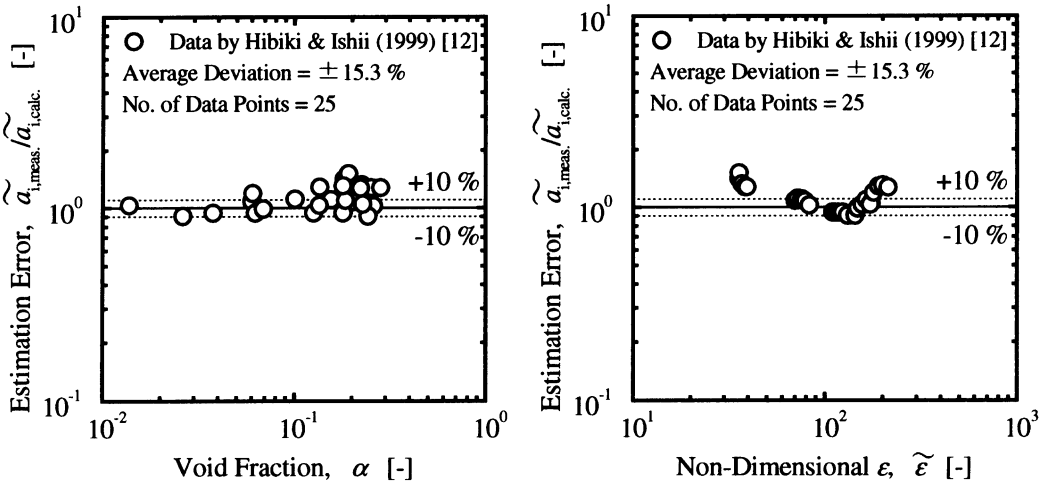


Fig. 2. Comparison of developed interfacial area correlation with data by Hibiki and Ishii [12].

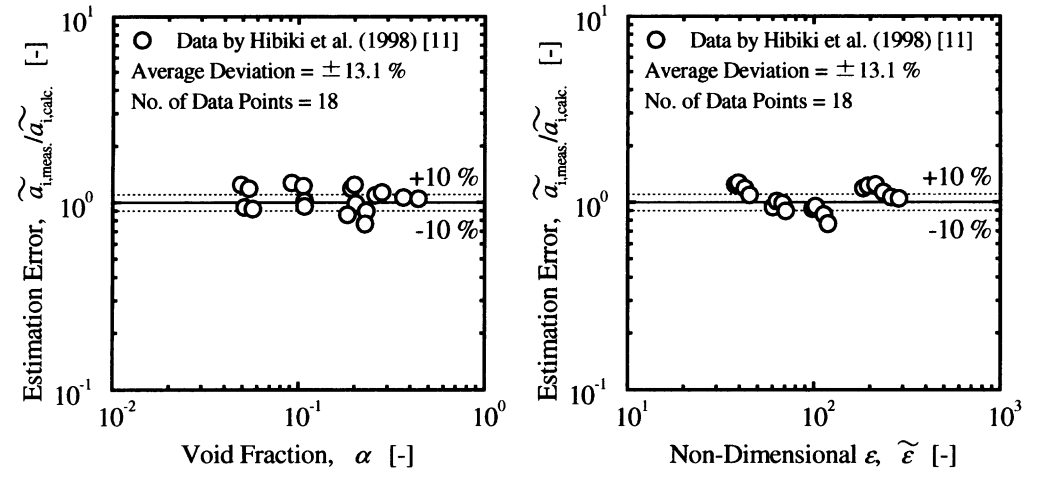


Fig. 3. Comparison of developed interfacial area correlation with data by Hibiki et al. [11].

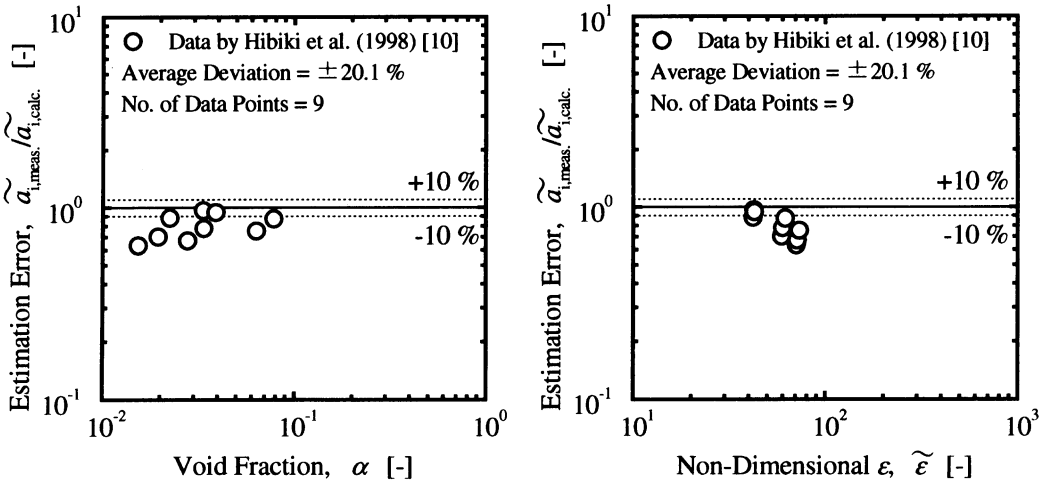


Fig. 4. Comparison of developed interfacial area correlation with data by Hibiki et al. [10].

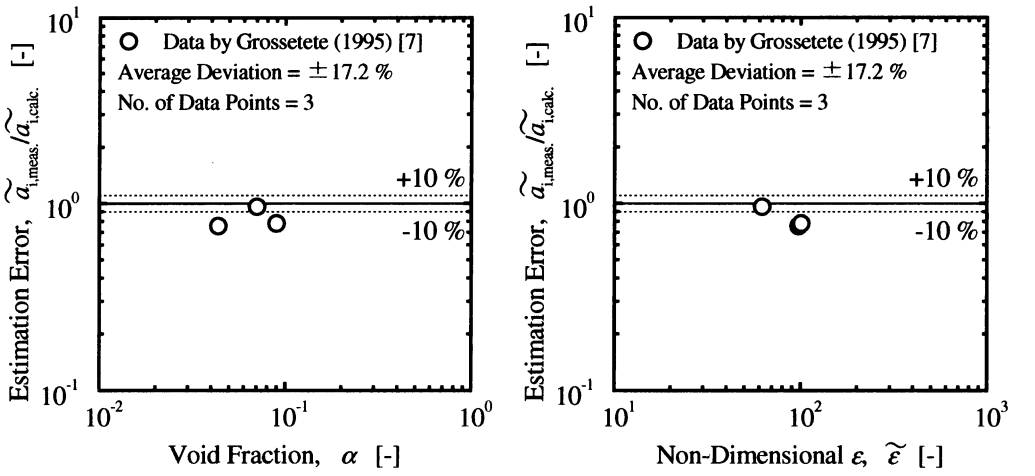


Fig. 5. Comparison of developed interfacial area correlation with data by Grossetete [7].

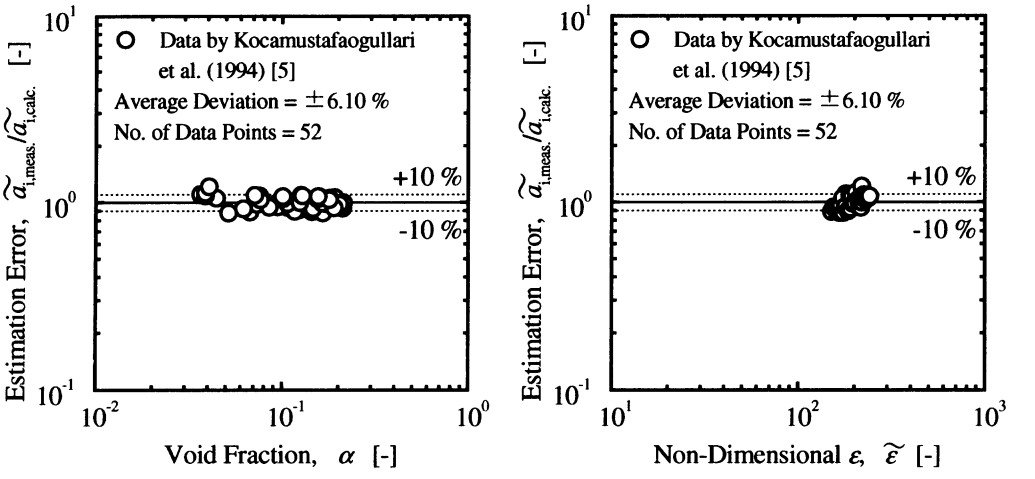


Fig. 6. Comparison of developed interfacial area correlation with data by Kocamustafaogullari et al. [5].

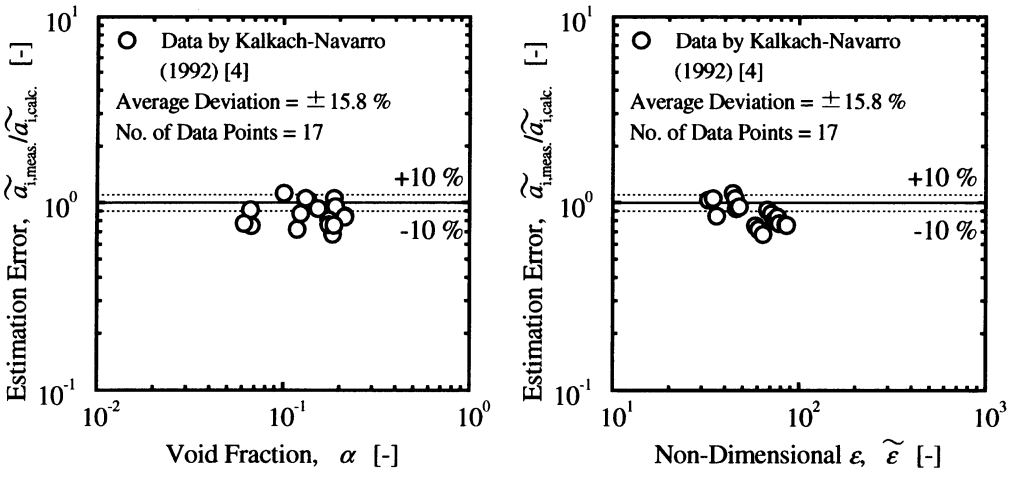


Fig. 7. Comparison of developed interfacial area correlation with data by Kalkach-Navarro [4].

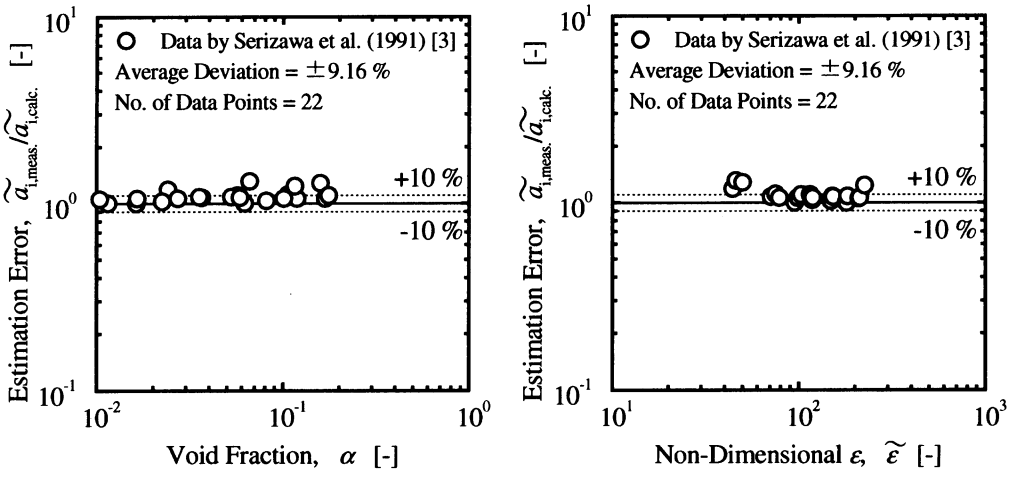


Fig. 8. Comparison of developed interfacial area correlation with data by Serizawa et al. [3].

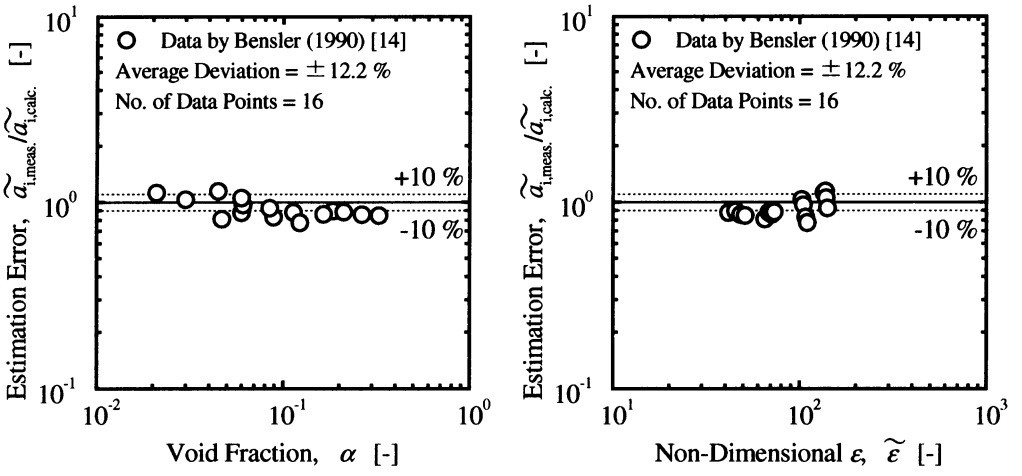


Fig. 9. Comparison of developed interfacial area correlation with data by Bensler [14].

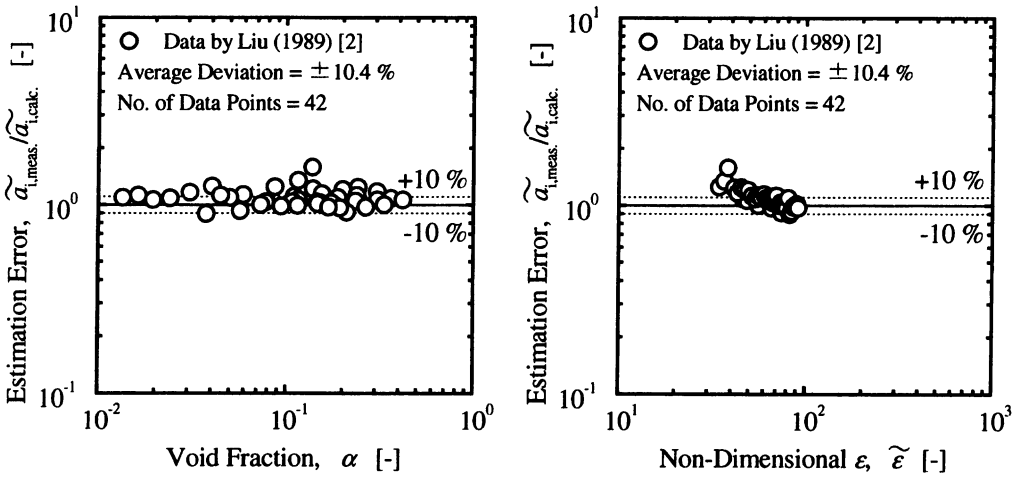


Fig. 10. Comparison of developed interfacial area correlation with data by Liu [2].

liquid velocity (0.262–6.55 m/s) and interfacial area concentration (25.8–1083 $m^{-1}$). The average relative deviation between Eq. (22) and the data is estimated to be ±11.1%.

For the condition of $\phi_{PN} \approx \phi_{PC}$, the present correlation, Eq. (22), may be applied approximately to even boiling flow. On trial, the present correlation is compared with the data taken in boiling water flows as shown in Figs. 11–13. Although the present correlation agrees with the data taken in a 3 × 3 bundle loop, an agreement between the present correlation and the data taken in an annulus loop and a 2 × 2 bundle loops is not satisfactory. This suggests that the bubble generation and collapse due to phase change should be considered in an interfacial area model to be developed in a future work.

Kocamustafaogullari et al. [5] developed the following theoretical model for interfacial area concentration based on the average pressure fluctuations generated by the turbulent liquid fluctuations acting across a bubble diameter and the competing surface tension forces. To finalize the model, Kocamustafaogullari et al. used their data obtained by the double sensor probe method with help of an equation derived by Kataoka et al. [47]. Recently, the equation by Kataoka et al. [47] has been improved as Eqs. (16) and (17) [10]. Taking account of this, the modified equation of Kocamustafaogullari et al. is expressed as

$$a_i = \frac{6\alpha\{j(-dP/dz)_F\}^{2/9}}{0.707(\sigma/\rho_f^{1/3})^{1/3}\{\alpha(1-\alpha)D_H^2\}^{2/9}}, \tag{26}$$

The original equation of Kocamustafaogullari et al. [5] is also given in Table 1. Interestingly, Eq. (26) can be recast as

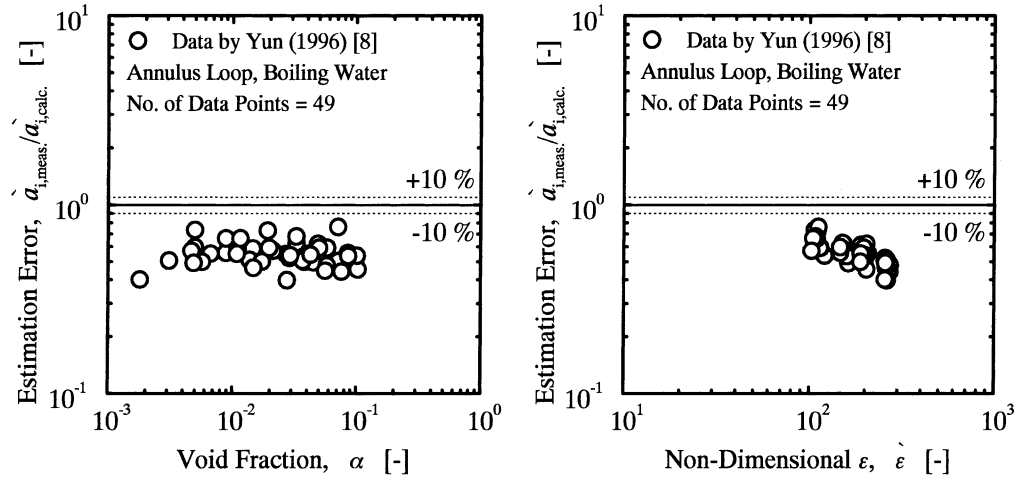


Fig. 11. Comparison of developed interfacial area correlation with data by Yun in annulus loop [8].

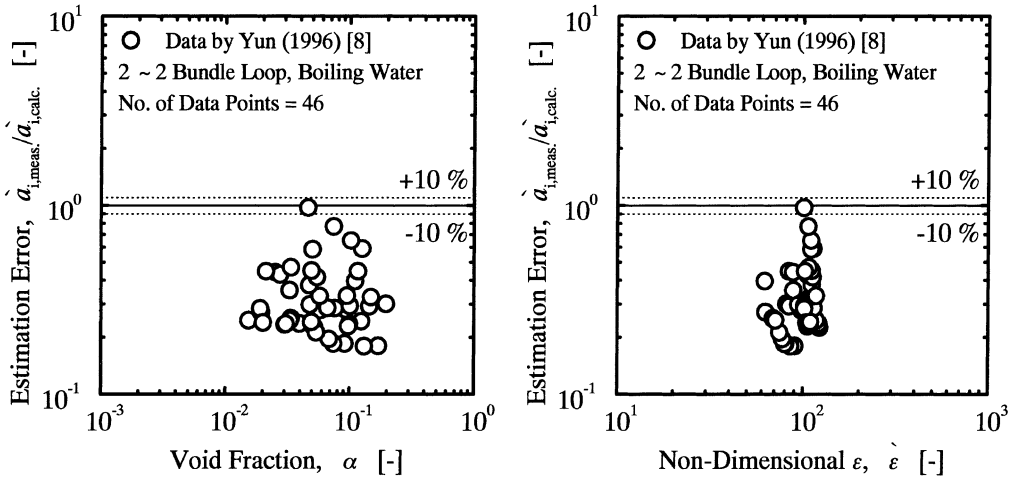


Fig. 12. Comparison of developed interfacial area correlation with data by Yun in $2 \times 2$ bundle loop [8].

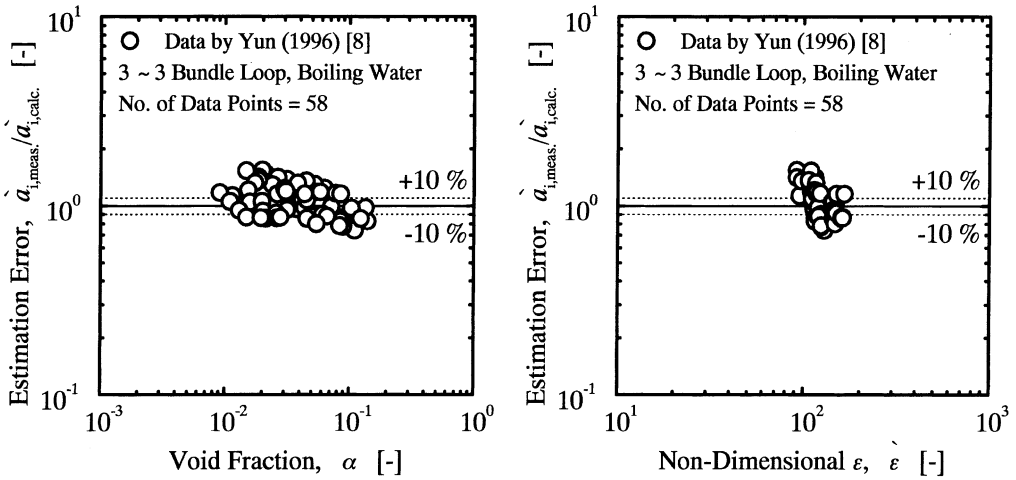


Fig. 13. Comparison of developed interfacial area correlation with data by Yun in $3 \times 3$ bundle loop [8].

$$a_i = (8.49 D_H^{-0.44}) \left( \frac{\sigma}{\rho_f} \right)^{-0.33} \alpha^{0.78} \varepsilon^{0.22}. \quad (27)$$

$$a_i = 5.41 \left( \frac{\sigma}{\rho_f} \right)^{-0.6} \alpha^{0.83} \varepsilon^{0.4}. \quad (28)$$

This functional form is similar to the interfacial area correlation developed in this study, Eq. (22). Fig. 14 shows the comparison of Eq. (26) with the data. For higher $\varepsilon$, Eq. (26) gives a good prediction of the interfacial area concentration. However, as $\varepsilon$ is decreased, the agreement becomes poor. Thus, the model of Kocamustafaogullari et al. [5] cannot be applied to low $\varepsilon$, since it was basically derived for horizontal bubbly flow where $\varepsilon$ is extremely high.

Millies et al. [21] also derived the interfacial area concentration theoretically from the Boltzmann transport equation for the probability density function of the bubbles under steady fully-developed conditions as

The functional form of this equation is very similar to Eqs. (9) or (10), which are derived theoretically for the case of very high or very low energy dissipation rate per unit mass, respectively. The exponent to $\alpha$ is also very similar to that in Eq. (22). Fig. 15 shows the comparison of Eq. (28) with the data. Unfortunately, Eq. (28) does not agree with the data satisfactorily. This may mainly be attributed to the overestimation of the exponent to $\varepsilon$ in Eq. (28).

The interfacial area correlation developed in this study, Eq. (22) has been validated by the database developed in adiabatic air–water bubbly flows so far ($25.4 \text{ mm} \leqslant D_H \leqslant 50.8 \text{ mm}$, $0.0178 \text{ m/s} \leqslant j_g \leqslant 4.87 \text{ m/s}$,

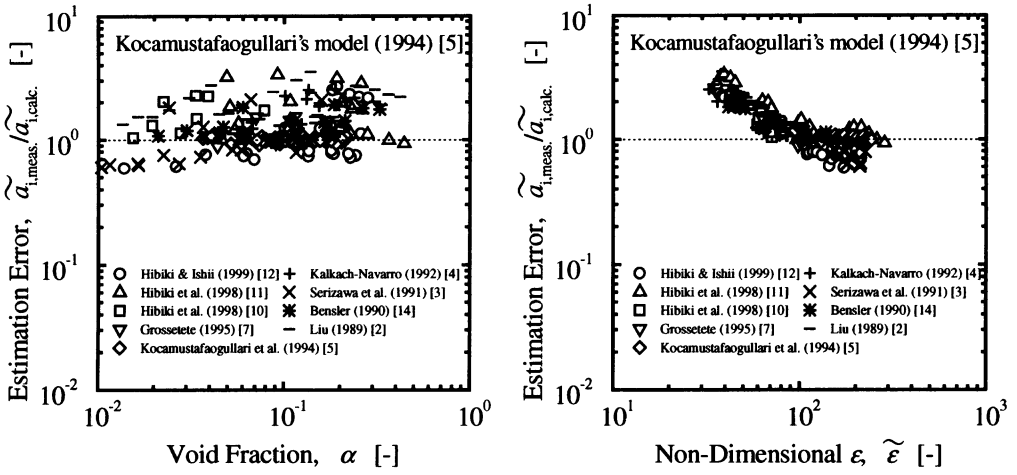


Fig. 14. Comparison of interfacial area model by Kocamustafaogullari et al. [5] with experimental data.

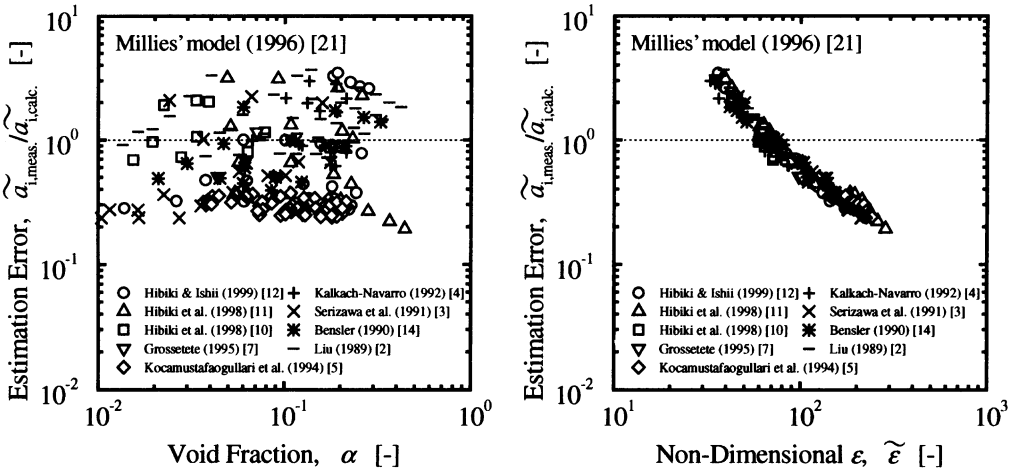


Fig. 15. Comparison of interfacial area model by Millies et al. [21] with experimental data.

$0.262\ \mathrm{m/s} \leqslant j_f \leqslant 6.55\ \mathrm{m/s}$, $25.8\ \mathrm{m^{-1}} \leqslant a_i \leqslant 1083\ \mathrm{m^{-1}}$). In order to apply the present correlation to other fluid systems, the coefficient and exponents may need to be modified based on extensive database, which will be developed in a future study.

## 4. Conclusions

Although bubbly flows are encountered in various engineering fields, there are very few established theoretical foundations on the interfacial area concentration, which have been supported by extensive experimental data. From this point of view, a simple equation for the interfacial area concentration under steady fully-developed flow condition has been derived from the interfacial area transport equation. The derived theoretical equation has been modified to obtain experimentally supported predictive correlation. Important conclusions obtained from this study are summarized below.

1. The correlation of the interfacial area concentration under steady fully-developed bubbly flow condition was derived from the interfacial area transport equation. The obtained equation was modified to obtain experimentally supported predictive correlation.
2. The obtained correlation of the interfacial area concentration, Eq. (22), was validated by 204 data sets measured in adiabatic air–water bubbly flows. These data sets covered extensive flow and loop conditions such as channel geometry (circular or rectangular

channel), flow direction (vertical or horizontal), superficial gas velocity (0.018–4.87 m/s), superficial liquid velocity (0.262–6.55 m/s) and interfacial area concentration (25.8–1083 $m^{-1}$). An excellent agreement was obtained within an average relative deviation of $\pm 11.1\%$.

3. Interfacial area models proposed by Kocamustafaogullari et al. [5] and Millies et al. [21] were compared with the data. For higher energy dissipation rate per unit mass, the interfacial area model proposed by Kocamustafaogullari et al. gave a good prediction of the interfacial area concentration. However, as the energy dissipation rate per unit mass was decreased, the agreement became poor. The interfacial area model proposed by Millies et al. could not reproduce the interfacial area concentration data.
4. The interfacial area correlation obtained in this study, Eq. (22), was compared with the data taken in boiling water flows. The result suggested that the introduction of bubble nucleation and collapse terms into the model would be indispensable for boiling flow.

## Acknowledgements

The authors would like to express their sincere appreciation to Professor Delhaye (CEA, Grenoble, France), Professor Park (Soul National University, Korea) and Professor Serizawa (Kyoto University, Japan) for providing valuable data sets. One of the authors (T. Hibiki) wishes to thank Prof. Hibiki (Tokyo Institute of Technology) for his continuous encouragement and support.

This work was performed under the auspices of the US Department of Energy's Office of Basic Energy Science. The authors would like to express their sincere appreciation for the encouragement, support and technical comments on this program from Drs. Manley, Goulard, and Price of DOE/BES. Part of this work was supported by grant-in-aid for Scientific Research from the Ministry of Education, Science, Sport and Culture (no. 12 780 385).

## References

[1] A. Serizawa, I. Kataoka, Phase distribution in two-phase flow, Transient Phenomena in Multiphase Flow, Hemisphere, Washington, DC, 1988, pp. 179–224.
[2] T.J. Liu, Experimental investigation of turbulence structure in two-phase bubbly flow, Ph.D. Thesis, Northwestern University, USA, 1989.
[3] A. Serizawa, I. Kataoka, I. Michiyoshi, Phase distribution in bubbly flow, in: G.F. Hewitt, J.M. Delhaye, N. Zuber (Eds.), Multiphase Science and Technology, vol. 6, Hemisphere, Washington, DC, 1991, pp. 257–301.
[4] S. Kalkach-Navarro, The mathematical modeling of flow regime transition in bubbly two-phase flow, Ph.D. Thesis, Rensselaer Polytechnic Institute, USA, 1992.
[5] G. Kocamustafaogullari, W.D. Huang, J. Razi, Measurement of modeling of average void fraction, bubble size and interfacial area, Nucl. Eng. Des. 148 (1994) 437–453.
[6] W.H. Leung, S.T. Revankar, Y. Ishii, M. Ishii, Axial development of interfacial area and void concentration profiles measured by double-sensor probe method, Int. J. Heat Mass Transfer 38 (1995) 445–453.
[7] C. Grossetete, Caracterisation experimentale et simulations de l'evolution d'un ecoulement diphasique a bulles ascendant dans une conduite verticale, Ph.D. Thesis, Ecole Centrale Paris, France, 1995.
[8] B.J. Yun, Measurement of two-phase flow parameters in the subcooled boiling, Ph.D. Thesis, Seoul National University, Korea, 1996.
[9] S. Hogsett, M. Ishii, Local two-phase flow measurements using sensor techniques, Nucl. Eng. Des. 175 (1997) 15–24.
[10] T. Hibiki, S. Hogsett, M. Ishii, Local measurement of interfacial area, interfacial velocity and liquid turbulence in two-phase flow, Nucl. Eng. Des. 184 (1998) 287–304.
[11] T. Hibiki, M. Ishii, Z. Xiao, Local flow measurements of vertical upward air–water flow in a round tube, Int. J. Heat Mass Transfer 44 (2001) 1869–1888.
[12] T. Hibiki, M. Ishii, Experimental study on interfacial area transport in bubbly two-phase flows, Int. J. Heat Mass Transfer 42 (1999) 3019–3035.
[13] J.M. Delhaye, P. Bricard, Interfacial area in bubbly flow: experimental data and correlations, Nucl. Eng. Des. 151 (1994) 65–77.
[14] H.P. Bensler, Détermination de l'aire interfaciale, du taux devide et du diameter moyen de Sauter dans un écoulement à bulles à partir de l'atténuation d'un faisceau d'ultrasons, Ph.D. Thesis, Institut National Polytechnique de Grenoble, France, 1990.
[15] P.H. Calderbank, Gas absorption from bubbles, Chem. Eng. 43 (1967) CE209–CE233.
[16] J. Burgess, P.H. Calderbank, The measurement of bubble parameters in two-phase dispersions – I, Chem. Eng. Sci. 30 (1975) 743–750.
[17] J. Burgess, P.H. Calderbank, The measurement of bubble parameters in two-phase dispersions – II, Chem. Eng. Sci. 30 (1975) 1107–1121.
[18] J. Burgess, P.H. Calderbank, The measurement of bubble parameters in two-phase dispersions – III, Chem. Eng. Sci. 30 (1975) 1511–1518.
[19] M.L. De Figueiredo, P.H. Calderbank, The scale-up of aerated mixing vessels for specified oxygen dissolution rates, Chem. Eng. Sci. 34 (1979) 1333–1338.
[20] K. Chandrasekharan, P.H. Calderbank, Further observations on the scale-up aerated mixing vessels, Chem. Eng. Sci. 36 (1981) 819–823.
[21] M. Millies, D.A. Drew, R.T. Lahey Jr., A first order relaxation model for the prediction of the local interfacial area density in two-phase flows, Int. J. Multiphase Flow 22 (1996) 1073–1104.
[22] M. Millies, D. Mewes, Interfacial area density in bubbly flow, Chem. Eng. Process. 38 (1999) 307–319.

[23] T. Hibiki, M. Ishii, One-group interfacial area transport of bubbly flows in vertical round tubes, Int. J. Heat Mass Transfer 43 (2000) 2711–2726.
[24] G. Kocamustafaogullari, M. Ishii, Foundation of the interfacial area transport equation and its closure relations, Int. J. Heat Mass Transfer 38 (1995) 481–493.
[25] Q. Wu, S. Kim, M. Ishii, S.G. Beus, One-group interfacial area transport in vertical bubbly flow, Int. J. Heat Mass Transfer 41 (1998) 1103–1112.
[26] L.B. Loeb, in: The Kinetic Theory of Gases, Dover, New York, USA, 1927.
[27] C. Tsouris, L.L. Tavlarides, Breakage and coalescence models for drops in turbulent dispersions, AIChE J. 40 (1994) 395–406.
[28] T. Oolman, H.W. Blanch, Bubble coalescence in air-sparged bioreactors, Biotech. Bioeng. 28 (1986) 578–584.
[29] T. Oolman, H.W. Blanch, Bubble coalescence in stagnant liquids, Chem. Eng. Commun. 43 (1986) 237–261.
[30] M.J. Prince, H.W. Blanch, Bubble coalescence and break-up in air-sparged bubble columns, AIChE J. 36 (1990) 1485–1497.
[31] O. Zeitoun, M. Shoukri, V. Chatoorgoon, Measurement of interfacial area concentration in subcooled liquid–vapour flow, Nucl. Eng. Des. 152 (1994) 243–255.
[32] Y. Hori, S. Toda, Condensation rate of vapour bubble in subcooled flow in a vertical tube, in: Proceedings of the International Conference on Multiphase Flows '91-Tsukuba, 1991, pp. 161–164.
[33] K. Tabei, M. Hasatani, M. Kuroda, Effective gas–liquid interfacial area in a mobile-bed contactor, Int. Chem. Eng. 29 (1989) 679–688.
[34] M. Fukuma, K. Muroyama, A. Yasunishi, Specific gas–liquid interfacial mass transfer coefficient in a slurry bubble column, J. Chem. Eng. Jpn. 20 (1987) 321–324.
[35] K. Viswanathan, Flow patterns in bubble, in: N.P. Cheremisinoff (Ed.), Encyclopedia of Fluid Mechanics, vol. 3, Gulf Publishing, 1985, pp. 1180–1215.
[36] P. Trambouze, H. van Laudeghem, J.P. Wauquier, Les réacteurs chimiques, Conception, calcul, mise en oeuvre, Publication de l'institut Français du Pétrole, Science et Technique du Pétrole, No. 26, Editions Technip, Paris, 1984 (Chapitre 8).
[37] J.E. Kelly, M.S. Kazimi, Interfacial exchange relations for two-fluid vapour–liquid flow: a simplified regime map approach, Nucl. Eng. Des. 81 (1981) 305–318.
[38] T. Tomida, F. Yusa, T. Okazaki, Effective interfacial area and liquid-side mass transfer coefficient in the upward two-phase flow of gas–liquid mixtures, Chem. Eng. J. 16 (1978) 81–88.
[39] G. Kasturi, J.B. Stepanek, Two-phase flow. III. Interfacial area in cocurrent gas–liquid flow, Chem. Eng. Sci. 29 (1974) 713–719.
[40] R.V. Shilimkan, J.B. Stepanek, Interfacial area in cocurrent gas–liquid upward flow in tubes of various size, Chem. Eng. Sci. 39 (1977) 149–154.
[41] K. Akita, F. Yoshida, Bubble size, interfacial area and liquid-phase mass transfer coefficient in bubble columns, Ind. Eng. Chem. Process Des. Dev. 13 (1974) 84–91.
[42] J.C. Japsen, Mass transfer in two-phase flow in horizontal pipelines, AIChE J. 16 (1970) 705–711.
[43] S. Banerjee, D.S. Scott, R. Rhodes, Studies on cocurrent gas–liquid flow in helically coiled tubes. II. Theory and experiments on turbulent mass transfer with and without chemical reaction, Can. J. Chem. Eng. 48 (1970) 542–551.
[44] P.H. Calderbank, Physical rate processes in industrial fermentation: part II. Mass transfer coefficients in gas–liquid contacting with and without mechanical agitation, Trans. Inst. Chem. Eng. 37 (1959) 173–185.
[45] R.W. Lockhart, R.C. Martinelli, Proposed correlation of data for isothermal two-phase two-component flow in pipes, Chem. Eng. Prog. 5 (1949) 39–48.
[46] J.W. Hinze, in: Turbulence, McGraw-Hill, New York, 1975.
[47] I. Kataoka, M. Ishii, A. Serizawa, Local formulation and measurements of interfacial area concentration in two-phase flow, Int. J. Multiphase flow 12 (1986) 505–529.